Investigation of the Structural, Thermal, Mechanical, and Optical Properties of Poly(methyl methacrylate) and Poly(vinylidene fluoride) Blends

S. M. Pawde, Kalim Deshmukh

Department of Physics, University Institute of Chemical Technology, University of Mumbai, Matunga, Mumbai 400019, India

Received 25 February 2008; accepted 2 March 2009
DOI 10.1002/app.30641
Published online 2 July 2009 in Wiley InterScience (www.interscience.wiley.com).

ABSTRACT: In this investigation, poly(methyl methacrylate) (PMMA) and poly(vinylidene fluoride) (PVDF) blends (w/w) were prepared in a Brabender (South Hackensack, NJ) plasticorder with a thermoplastic mixing chamber (type W60) preheated at 180°C. These blends were further converted into films by a conventional solution casting method and characterized with Fourier transform infrared spectroscopy, differential scanning calorimetry, X-ray diffraction, mechanical property measurements, impact strength testing, ultraviolet–visible spectroscopy, refractive-index measurements, and contact-angle study. The Fourier transform infrared results indicated that the compatibility between these two systems resulted from hydrogen bonding between the carbonyl group of PMMA and the CH_2 group of PVDF. The thermal analysis showed depressions in the glass-transition temperature, melting temperature, and crystallization temperature. The heat of crystallization increased with an increase in the PVDF content in the blend. An increase in the heat of crystallization meant an increase in the crystallinity. An increase in the cooling rate increased the crystallization rate. The improvement in the mechanical properties of the blend films indicated that the observed behavior was ascribable to a more coherent structure of the blends due to strong specific interactions between PMMA and PVDF chains. The impact strength analysis revealed a substantial increase in the impact strength from 21.64 to 38.52 J/m. Optical absorption spectra suggested the presence of an optical band gap energy that increased with an increase in the PVDF content in the blend. The contact angle against water increased with the PVDF content in the blend film, and this was caused by the hydrophobicity of PVDF due to the CF_2 group of PVDF. © 2009 Wiley Periodicals, Inc. J Appl Polym Sci 114: 2169–2179, 2009

Key words: blends; compatibility; differential scanning calorimetry (DSC); FT-IR

INTRODUCTION

The importance of polymer blending has increased in recent years because of the preparation of polymeric materials with desirable properties, low costs, and improved processability. Polymer blends are physical mixtures of structurally different polymers or copolymers that interact through secondary forces with no covalent bonding and are miscible at the molecular level. Polymer blends are an important class of materials specifically designed and used for applications that take advantage of the enhanced properties offered by properly fabricated materials. The study of polymer blends has undergone rapid development in recent years and is one of the more advanced domains in modern polymer science. Blend systems that are composed of existing materials can be developed at reduced cost to suit new market requirements.[1] Because the properties of a blend system vary with the composition, an existing blend can be easily and quickly modified to meet performance and cost objectives required for new or changing markets. New blend systems are particularly attractive when one of the components is much less expensive than the others because this allows the blend to be produced at a low cost. Blends also can be commercially rewarding if they improve processability and performance. Other advantages of polymer blending are versatility; simplicity, and inexpensiveness.[2] The general morphologies and final blend properties depend not only on the individual properties of blend components but also on their degree of miscibility.[3] However, most polymer systems are immiscible, and only limited polymer pairs are partially miscible within specific temperature ranges and with specific component concentrations. Therefore, the study of miscibility has received great attention in polymer blends because of the technological applications of these materials.

The miscibility of poly(methyl methacrylate) (PMMA)/poly(vinylidene fluoride) (PVDF) blends has been studied extensively and has been evaluated by means such as the transparency of the blends, the

Correspondence to: S. M. Pawde (sunita_pawde@yahoo.com).

Flory–Huggins interaction parameter, and the glass-transition temperature (T_g). These blends marry the chemical flame resistance, toughness, and piezoelectric nature of PVDF[4,5] with the modulus, tensile strength, low smoke toxicity, and optical properties of PMMA.[6] Because of their superior barrier properties, such as the chemical/flame resistance and toughness/flexibility of PVDF,[7] along with the hardness, rigidity, low smoke toxicity, and superior transmission/refractive[8] properties of PMMA, these blends are of considerable commercial relevance. The characteristics and morphology of PMMA/PVDF blends have been investigated with various techniques such as X-ray, Fourier transform infrared (FTIR), optical, calorimetric, microscopic, and electrical measurements.[9–12] PMMA/PVDF blends are examples of miscibility between an amorphous polymer (PMMA) and a semicrystalline polymer (PVDF). The blends have been found to be completely miscible over the entire composition range above the PVDF melting temperature (T_m) of 170°C and below the lower critical solution temperature of 330°C. The apparent compatibility of these two polymer is due to some specific interaction (e.g., complex formation) between the individual PVDF and PMMA chains.

Since its discovery, PVDF has been the center of scientific attention in polymer science. It is a semicrystalline polymer that has at least four types of crystalline structures, which are known as the α, β, γ, and δ phases.[13,14] The α form can be produced during crystallization from the melt easily. The polar phases β and γ are technologically the most interesting because of their better pyroelectric and piezoelectric properties. The β crystal in PVDF can be obtained by mechanical deformation, poling under a high electric field, or crystallization from the melt under high pressure or at very high cooling rates.[15,16] PVDF can be easily processed and has excellent mechanical properties, high chemical resistance, good thermal stability, and high pyroelectric and piezoelectric properties. These properties provide a wide range of scientific and technological applications[17,18] ranging from simple protective coatings for pipes and buildings to transducer devices, detectors, and ferroelectric memories.

PMMA is a versatile polymer with wide commercial applications that exhibits good mechanical properties and outdoor weathering. It is one of the most important acrylic polymers widely used because of its excellent optical clarity and its possible use in nonlinear optics. The use of PMMA is well known because it is a hard and rigid polymer. PMMA is used in outdoor electrical applications, high-voltage applications, transparent neutron stoppers, standard broadcast television waves, radar band magnifiers, and automotive tail lights because of its good compatibility with other polymers, high resistance, surface resistance, and optical properties. It exhibits some specific properties such as optical absorption in the visible domain, light weight, good chemical stability, good processability, an ability to insulate, simple synthesis, and low cost. The most common method for promoting the toughness of PMMA is blending and copolymerization. PMMA/PVDF blends are examples of amorphous/crystalline polymer blends, and the nature and characteristics of such amorphous/crystalline polymer blends are well accepted.[19]

The main objective of this work was to develop and understand the necessary thermodynamic background to prepare polymer blends. The second was to assess the compatibility and miscibility of the blends. The third objective was to assess the effect of the blend composition on the degree of crystallinity. Hence, with this interest, PMMA/PVDF blends of different compositions were prepared. The compatibility of these two polymers was evaluated with analytical techniques such as FTIR spectroscopy, differential scanning calorimetry (DSC), X-ray diffraction (XRD), mechanical property measurements, impact strength testing, and ultraviolet–visible (UV–vis) spectroscopy. The contact angles of PMMA/PVDF blend films and the refractive indices of the blend solutions were also studied.

EXPERIMENTAL

Materials

PMMA and PVDF were received in research grade (RG) granules from IPCL (Baroda, India) and Kureha Chemical Industry Co., Ltd. (Tokyo, Japan), respectively. Dimethylformamide was obtained from S.D. Fine Chemicals, Ltd. (Mumbai, India).

Blend preparation

Blends of PMMA and PVDF with different compositions (90/10, 80/20, 70/30, 60/40, and 50/50 w/w) were prepared in a Brabender plasticorder with a thermoplastic mixing chamber (type W60) preheated at 180°C. The rotor speed was set at 60 rpm. Ten minutes of mixing was enough to generate a steady-state torque response, which indicated a uniform dispersion of the components.

Film preparation

The blends obtained with the Brabender plasticorder were further converted into films by dissolution in dimethylformamide at 60°C. This solution was put aside to obtain a suitable refractive index, and then the solution so obtained was poured onto a cleaned glass Petri dish and kept in an oven at 60°C for slow evaporation of the solvents. The solution was evaporated completely, and a thin film of the PMMA/

PVDF blend remained on the Petri dish. These films were peeled from the plate and kept in vacuum desiccators for further study.

Characterization

The refractive index was measured with an Abbe digital multiwavelength refractometer (Milton Roy Co., Ivyland, PA) for PMMA/PVDF blend solutions of different compositions.

FTIR spectroscopy of PMMA/PVDF blend films 40–50 μm thick was performed with an attenuated total reflection FTIR spectrophotometer (Paragon 500, PerkinElmer, Beaconsfield, United Kingdom) in the wave-number range of 400–3500 cm^{-1} with a resolution of 4 cm^{-1}. The FTIR spectra were taken in the transmittance mode.

The thermal analysis of PMMA/PVDF blends was performed with a PerkinElmer (Norwalk, CT) DSC-7 differential scanning calorimeter operating on a UNIX platform at a heating rate of 10°C/min under a nitrogen flow of 0.5 kg/cm^2 in the temperature range of 50–300°C. The heat of crystallization was determined from the area of the exothermic peak during cooling, and $t_{1/2}$ was defined as the half-time between the crystallization onset time and the crystallization ending time.

XRD of PMMA/PVDF blend films 40–50 μm thick was recorded with a Bruker D8 advance XRD meter (Rigaku, Tokyo, Japan) with Ni-filtered Cu Kα radiation (wavelength = 1.54060 Å) with a graphite monochromator. The scans were taken in the 2θ range of 4–80° with a scanning speed and step size of 1°/mm and 0.01°, respectively. The crystallinity percentage was measured with a formula given elsewhere.[20]

The mechanical properties of PMMA/PVDF blend films 40–50 μm thick were tested on a Lloyd LR10K universal tensile machine (Lloyd Instruments Limited, Hampshire, England). A thin film 4 cm long and 1 cm wide (ASTM D 638) was gripped between the two jaws of the tensile machine. The crosshead speed was kept at 5 mm/min. The average value was calculated from a set of at least 10 repeats.

The impact strength tests of PMMA/PVDF blend films 40–50 μm thick were performed on an Izod Charpy digital impact tester (ATS FAAR, Ceast, Segrate, Italy). The specimens used for impact strength testing were 63.5 mm × 12.5 mm with a notched radius of 0.25 mm (ASTM D 256). The average value was calculated from a set of at least 10 repeats.

UV–vis absorption spectra of PMMA/PVDF blend films 40–50 μm thick were obtained with a PerkinElmer Lambda/25/35/45 UV–vis spectrophotometer in the range of 200–600 nm.

The contact angles of PMMA/PVDF blend films 40–50 μm thick were measured by the sessile drop method. The contact angle was determined at 10 different places for the same sample, and an average value was determined with an error of ±1.4°.

RESULTS AND DISCUSSION

Refractive-index measurements

In general, the measurement of the refractive index of a polymer solution is more accurate and simpler to perform than the determination of its density. There has been considerable demand for high-performance, high-refractive-index materials in recent years because of their widespread applications in optical devices. In this study, refractive indices of PMMA/PVDF blend solutions of different compositions were measured, and they are depicted in Figure 1. As the percentage of PVDF in the blends increased, there was a linear decrease in the refractive index. It was expected that the light transmittance of PMMA would be reduced gradually by the addition of semicrystalline PVDF. The decrease in the refractive index of the blend solutions was interpreted as an indication of decreasing molecular orientation in the PMMA/PVDF blends due to the addition of PVDF to PMMA.

FTIR spectroscopy

Normally, IR spectroscopy of blends is carried out to explore the possible interactions between the blend components. In this study, we performed FTIR spectroscopy with the same aim of ascertaining possible interactions between the PMMA and PVDF chains. Figure 2 displays IR spectra of PMMA, PVDF, and blends of different compositions. Figure 2(a) shows the FTIR spectrum of pure PMMA, which displays various bands. The bands at 2992, 2954, and 2951 cm^{-1} are assigned to the CH_2, C—O—CH_3, and CH stretching vibrations,[21] whereas the bands at 1733 and 1433 cm^{-1} are assigned to the stretching

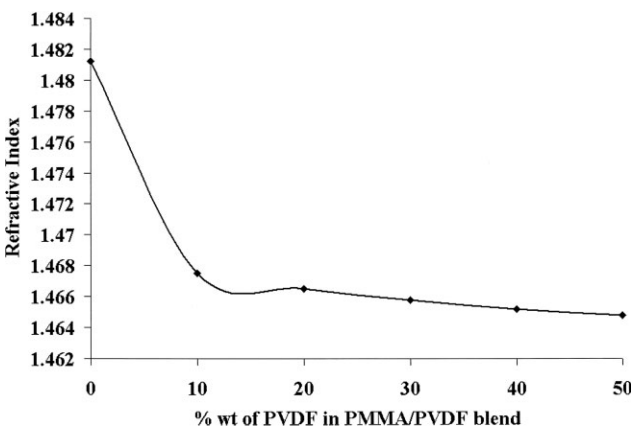

Figure 1 Variation in the refractive index for PMMA/PVDF blends of different compositions.

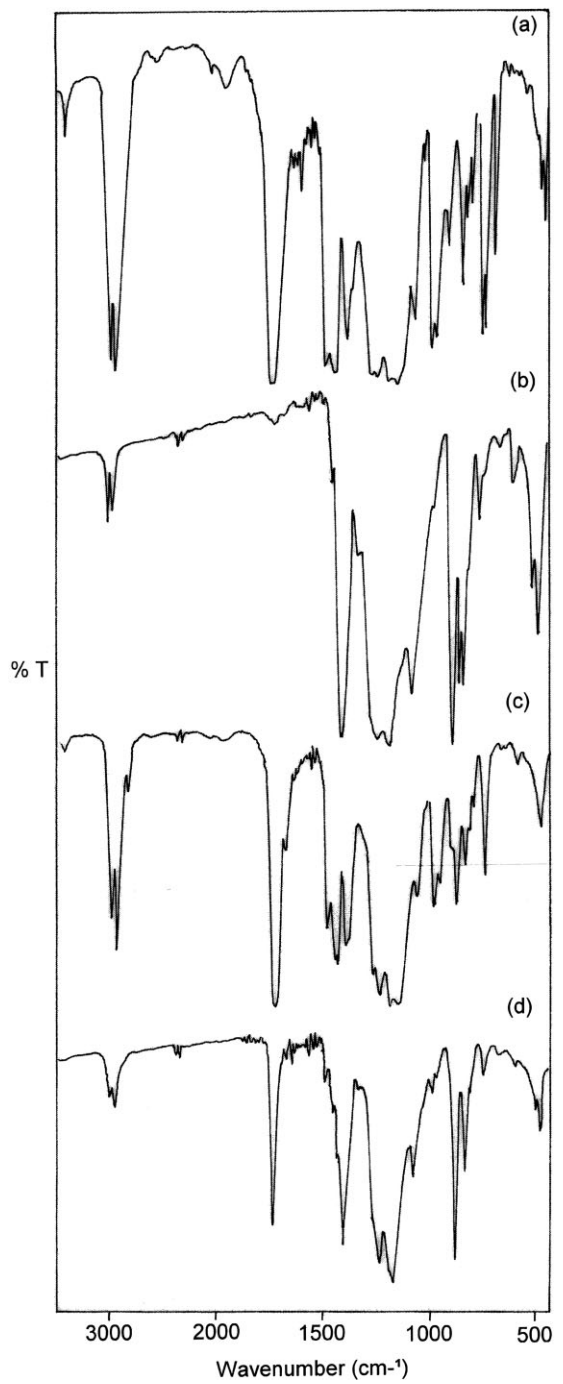

Figure 2 FTIR spectra for PMMA/PVDF blends of different compositions: (a) pure PMMA, (b) pure PVDF, (c) 90/10 PMMA/PVDF, and (d) 80/20 PMMA/PVDF.

vibrations of C=O and —O—CH_3 groups of PMMA.[22] The bands at 1485, 1173, and 947 cm^{-1} are assigned to CH_2 scissoring, twisting, and wagging modes of PMMA, whereas the bands at 750 and 736 cm^{-1} are assigned to the CH_2 rocking mode of PMMA.[22] The band at 1250 cm^{-1} is assigned to the C—O stretching vibration of PMMA. The bands at 1388 and 1159 cm^{-1} are assigned to O—CH_3 stretching,[21,23] whereas the bands at 1630, 1300, and 1330 cm^{-1} are assigned to C=O stretching and CH_2 stretching vibrations.[24] Very distinctive absorption bands can be observed at 1743 and 1187 cm^{-1}, and these are due to the C=O and C—O stretching of the ester group of PMMA. The appearance of the stretching absorption band at 1373 cm^{-1} confirms the presence of the methyl group of PMMA.[25]

Figure 2(b) shows the FTIR spectrum of PVDF, which gives more information about the crystalline phase of PVDF. A careful analysis of the FTIR spectrum of PVDF suggests that a typical vibrational band observed at 1404 cm^{-1} corresponds to the deformed vibration of the CH_2 group,[22] whereas those peaks appearing at 1233, 1176, and 1072 cm^{-1} may be assigned to C—F and CF_2 stretching modes of vibrations. The bands observed at 881 and 840 cm^{-1} are assigned to the characteristic frequency of the vinylidene compound.[22,29] The absorption band seen at 512 and 481 cm^{-1} can be attributed to the wagging and bending vibrations of CF_2, respectively.[30] The characteristic absorption bands observed at 481, 531, 612, 766, 795, 855, and 976 cm^{-1} are assigned to the α phase of PVDF, and the bands at 470, 512, and 840 cm^{-1} are assigned to the β phase of PVDF.[31] Also, the band observed at 3021 cm^{-1} corresponds to the β phase of PVDF. The peak assignments for the FTIR spectra of PMMA and PVDF are given in Table I.

Figures 2(c,d) and 3(e–g) show the FTIR spectra of PMMA/PVDF blends with different compositions. It is clear that the stretching frequency at 1733 cm^{-1}, which corresponds to the C=O group of PMMA, is shifted to the higher wavelength side in all the blends. This shift in the carbonyl stretching frequencies of the blends, in comparison with pure PMMA, is due to a specific interaction between the carbonyl group of PMMA and the CH_2 group of PVDF, which indicates the proper formation of the blends of the two components. The energy gained from the mixing of the two polymers is partly attributed to interactions between the PMMA carbonyl group and the electric moment of PVDF monomer units and to hydrogen bonding between the PMMA carbonyl oxygen and the PVDF protons.

Thermal analysis

The thermal behavior of polymers is interesting as their structure and crystallization are very sensitive to temperature. The determination of T_g is a widely used method to study miscibility in polymer blends. T_g is the characteristic temperature of any polymer at which the polymeric system changes from a hard and glassy state to a flexible, rubbery state. This happens because of the segmental motion of the polymeric chains.

TABLE I
Peak Assignments for PMMA and PVDF

PVDF peak position (cm^{-1})	Peak assignment	PMMA peak position (cm^{-1})	Peak assignment
1186	CF_2 stretching[22]	1250	C=O stretching[22]
1404	CH_2 deformation[22]	1630	C=O stretching[24]
1072	CF_2 stretching[29]	1300	CH_2 stretching[24]
1176	CF stretching[29]	1330	CH_2 stretching[24]
1233	CF stretching[29]	1439	CH_3 stretching[26,27]
512	CF_2 wagging[30]	1700–1744	C=O stretching[26,27]
481	CF_2 bending[30]	950–650	C—H bending[28]
531	CF_2 bending[31]	1260–1000	C—O stretching[28]
845	CH_2 rocking[31]	3000–2900	C—H stretching[28]

In this study, we performed a thermal analysis to reveal the glass-transition behavior in the PMMA/PVDF blends. The DSC results provided evidence of a single T_g for the blends of various compositions.

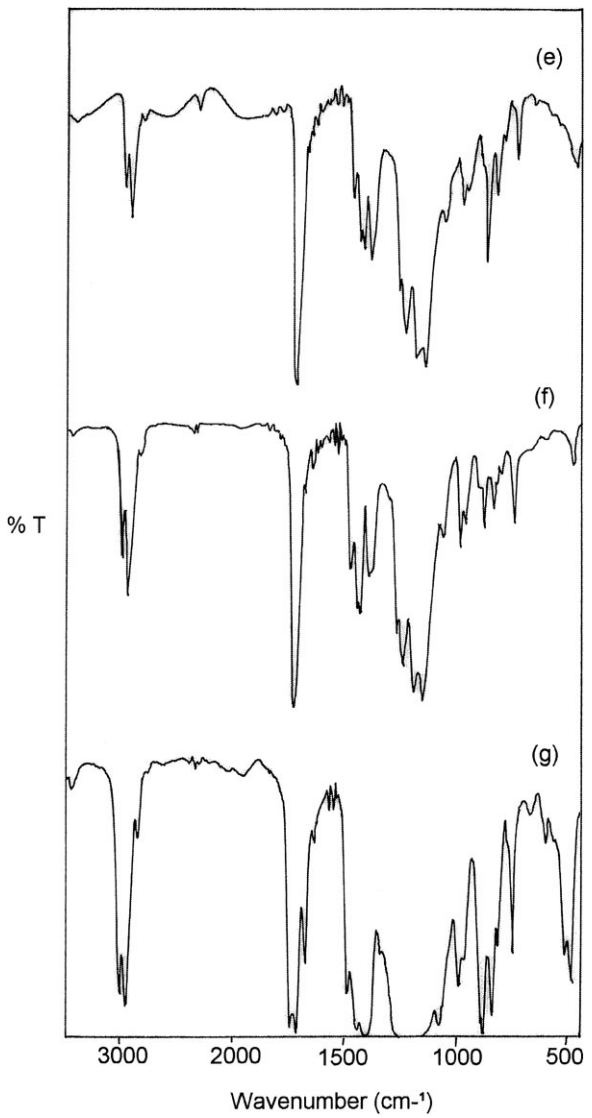

Figure 3 FTIR spectra for PMMA/PVDF blends of different compositions: (e) 70/30, (f) 60/40, and (g) 50/50.

Table II shows that as the percentage of PVDF in the blend increased, T_g decreased up to 55.21°C. Thermal evidence in addition to the blend T_g includes T_m, and the melting point depression is generally discussed to evaluate interactions.

The DSC melting thermograms for PMMA/PVDF blends of different compositions are shown in Figure 4. An endothermic peak corresponding to the melting of pure PVDF can be observed at 166.59°C [Fig. 4(a)], and a melting peak for pure PMMA can be observed at 160.23°C [Fig. 4(b)]. The remaining blend compositions showed melting peaks at 164.36, 161.42, 159.74, 157.13, and 155.51°C, as shown in Figure 4(c–f). The melting peaks for all the blend compositions were lower than that of the pure PVDF. The values observed for T_m could be due to either the higher percentage of crystallinity or the cross-linking of PMMA chains with PVDF.

The recording of the DSC scan during cooling enabled us to observe the crystallization temperature (T_c). It can be noted from Figure 5 that T_c decreased from 144.28°C for pure PVDF to 136.23°C for the 50/50 blend composition. The behavior of T_g, T_m, and T_c for PMMA/PVDF blends of different compositions is shown graphically in Figure 6. These results show that the incorporation of PVDF in the PMMA matrix made the blends thermally more stable. The heat of crystallization increased with an increase in

TABLE II
DSC Results for PMMA/PVDF Blends of Different Compositions

PMMA/PVDF blend	T_g (°C)	T_m (°C)	T_c (°C)	Heat of crystallization (J/g)
PMMA	109	160.23	—	63.4
PVDF	—	166.59	144.28	76.8
90/10	96.56	164.36	176.12	65.3
80/20	83.25	161.42	172.12	68.5
70/30	74.06	159.74	170.16	70.3
60/40	62.61	157.13	165.16	71.9
50/50	55.21	155.51	160.23	73.2

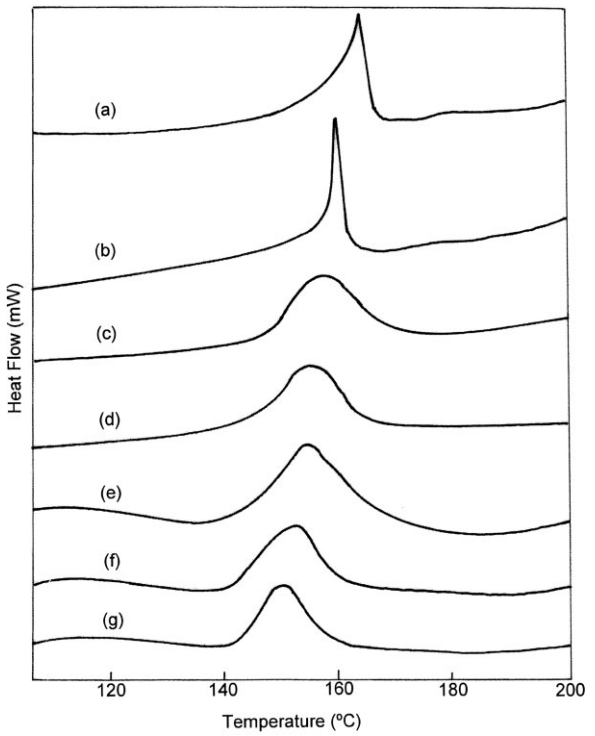

Figure 4 Melting thermograms for PMMA/PVDF blends of different compositions: (a) pure PVDF, (b) pure PMMA, (c) 90/10 PMMA/PVDF, (d) 80/20 PMMA/PVDF, (e) 70/30 PMMA/PVDF, (f) 60/40 PMMA/PVDF, and (g) 50/50 PMMA/PVDF.

the PVDF content. Figure 7 shows the influence of the PVDF content on the heat of crystallization. The increase in the heat of crystallization meant an increase in the crystallinity.[32] With an increase in the PVDF content in the blend, the chance of contact between PMMA and PVDF molecules became higher, and this led to high crystallinity.[33] Figure 8 reflects the influence of cooling rates on $t_{1/2}$. $t_{1/2}$ presents the overall crystallization rate; that is, the shorter $t_{1/2}$ is, the faster the overall crystallization rate is. With the cooling rate increasing, $t_{1/2}$ decreased. The explanation is that two factors, the nucleation and growth rate of crystallization, control the overall crystallization rate. Increasing the cooling rate can raise the nucleation density and increase the nucleation rate but reduce the growth rate. In general,[34] the increase in the nucleation rate is faster than the decrease in the growth rate as the cooling rate increases. Thus, the cooling rate increase will result in an increase in the overall crystallization rate.

XRD

XRD is a useful tool for investigating the crystalline forms of the blends. Figure 9(a,b) shows typical XRD spectra corresponding to pure PVDF and pure PMMA. The interplanar distances (d values), 2θ val-

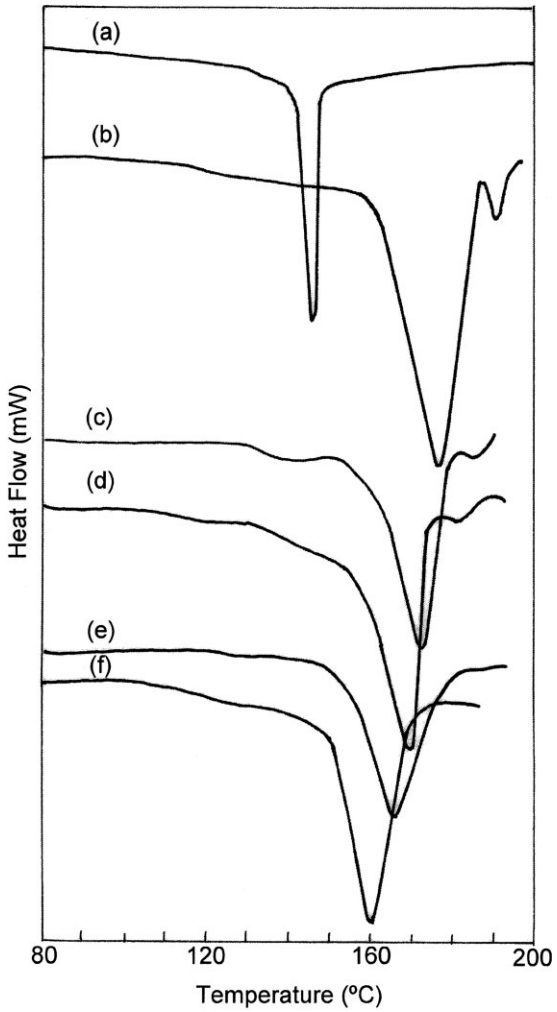

Figure 5 Crystallization thermograms for PMMA/PVDF blends of different compositions: (a) pure PVDF, (b) 90/10 PMMA/PVDF, (c) 80/20 PMMA/PVDF, (d) 70/30 PMMA/PVDF, (e) 60/40 PMMA/PVDF, and (f) 50/50 PMMA/PVDF.

ues, and crystallinity (%) of the PMMA/PVDF blends are listed in Table III. From Figure 9(a), it is clear that PVDF is characterized by relatively sharp

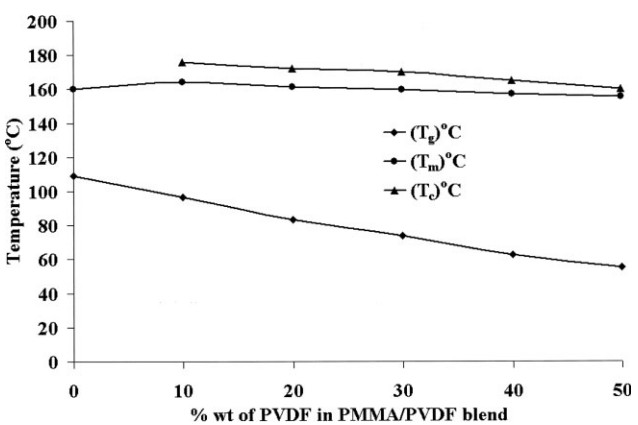

Figure 6 Variation in T_g, T_m, and T_c for PMMA/PVDF blends of different compositions.

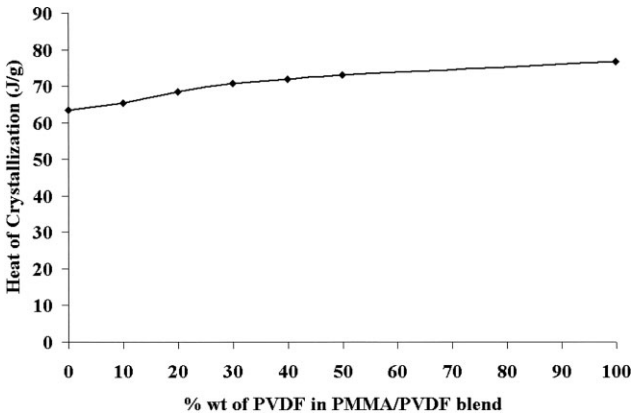

Figure 7 Relationship between the PVDF content in the blend and the heat of crystallization (cooling rate = 10°C/min).

diffraction peaks at $2\theta = 15.09$ and $2\theta = 26.7$, which are attributed to the crystal planes associated with the α phase of PVDF.[35,36] The monoclinic form, the β form with piezoelectric and pyroelectric properties, does not obviously occur. These results show that the crystalline form, which remains mainly α phase in pure PVDF and all PMMA/PVDF blends,[16,37,38] is not changed after blending with PMMA. From Figure 9(b), it is clear that pure PMMA has an amorphous nature characterized by an amorphous halo (a large hump) at $2\theta = 14.56°$ with no sharp peak. This shows that it is a glassy material because of the absence of a crystalline peak.[2]

XRD spectra corresponding to PMMA/PVDF blends of different compositions are shown in Figure 10. All the blend samples showed one large hump, which provided a clear indication of the complexation of the two polymer blends. The XRD scans of the blends show that the increase in the PVDF content of the blends increased the area under the peak; this indicated an increase in the crystallinity. The *d*-spacing values decreased from 6.047 to 5.117 Å as the PVDF content in the blend increased, whereas

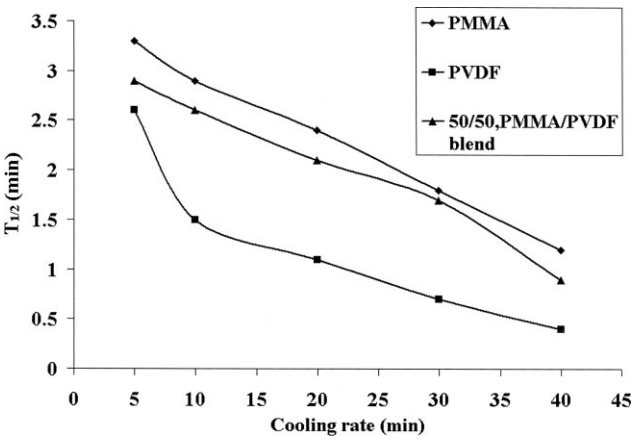

Figure 8 Relationship between $t_{1/2}$ and the cooling rate.

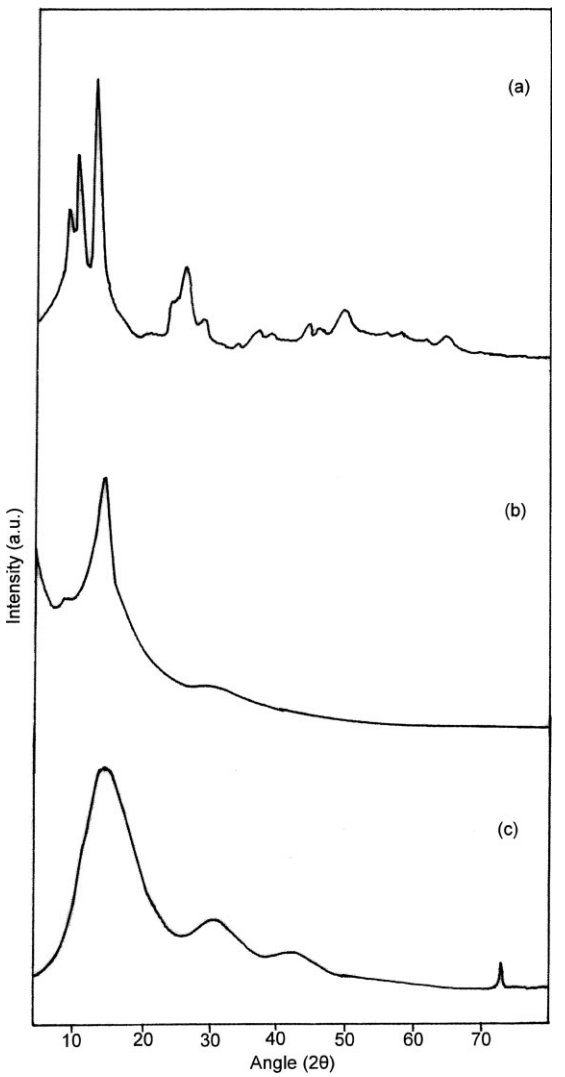

Figure 9 XRD for PMMA/PVDF blends of different compositions: (a) pure PVDF, (b) pure PMMA, and (c) 90/10 PMMA/PVDF.

TABLE III
XRD Results, Optical Band Gap Energy Values, and Contact Angles for PMMA/PVDF Blends of Different Compositions

PMMA/PVDF blend	2θ	*d* (Å)[a]	Crystallinity (%)	Activation energy (eV)	Contact angle (°)
PMMA	14.560	6.083	33.71	3.74	80.12
PVDF	15.095	5.869	51.94	5.32	102.21
90/10	14.674	6.047	43.83	4.19	84.23
80/20	15.702	5.643	45.51	4.28	88.02
70/30	16.555	5.354	47.29	4.42	90.52
60/40	16.730	5.308	48.63	4.57	93.42
50/50	17.320	5.117	49.38	4.63	96.09

[a] $d = n\lambda/2 \sin\theta$, where λ is the wavelength, *n* is an integer determined by the order given, and θ is the angle between the incident ray and the scattering planes.

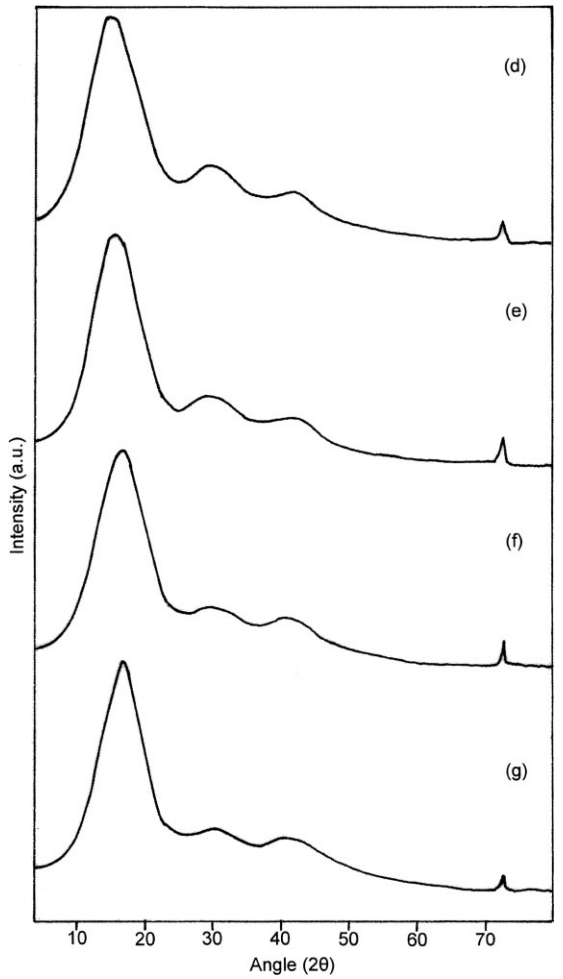

Figure 10 XRD for PMMA/PVDF blends of different compositions: (d) 80/20, (e) 70/30, (f) 60/40, and (g) 50/50.

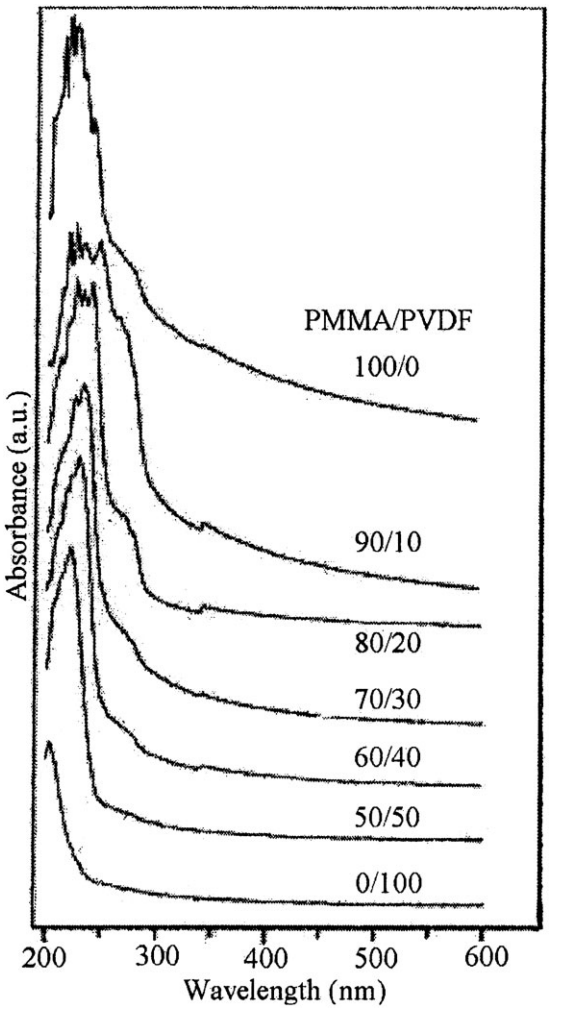

Figure 11 UV–vis spectra for PMMA/PVDF blend films of different compositions.

the angle (2θ) values decreased. The decrease in the *d* value showed an induction of stress due to PMMA. The reason for such stress can be understood on the basis of the intermolecular interactions of PMMA with fluorine of PVDF. Thus, the XRD analysis reveals that blending occurred on the basis of the influence of PVDF on PMMA in the blends.

UV–vis spectra

UV–vis absorption spectra of PMMA/PVDF blends are shown in Figure 11. The absorption bands were observed in the region of 220–270 nm. The sharp absorption edge for PVDF indicated the semicrystalline nature of PVDF. A shift in the absorption band toward a higher wavelength with a different absorption intensity was observed for the PMMA/PVDF blend films. These shifts indicated the formation of intramolecular interactions between PMMA and PVDF, and this supported the FTIR and XRD results. Also, the shift in the absorption edge in the films reflected the variation in the optical band gap energy. It is clear that some of the blends exhibited a well-defined window in the wavelength range of 270–350 nm. A sharp and maximum height of this window was observed for the 70/30 composition of the blend. This optical window can be used as an

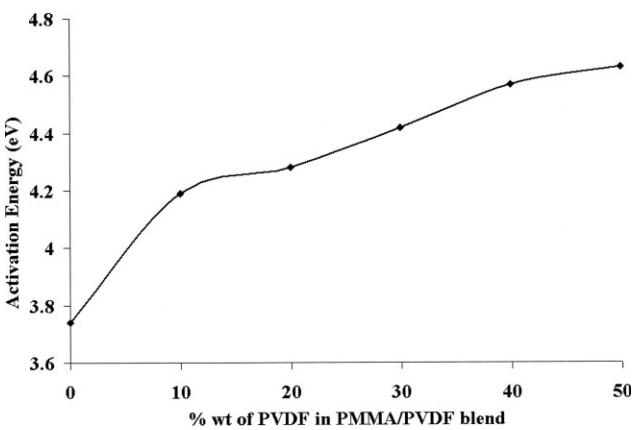

Figure 12 Optical band gap energy of PMMA/PVDF blend films.

TABLE IV
Mechanical Properties of PMMA/PVDF Blends of Different Compositions

PMMA/PVDF blend	Tensile strength (MPa)	Elongation (%)	Young's modulus (MPa)	Impact strength (J/m)
PMMA	3.064	5.681	5.735	21.64
PVDF	43.691	7.292	15.936	50.44
90/10	3.516	6.263	10.463	23.43
80/20	5.724	7.886	12.526	27.16
70/30	6.542	9.015	12.578	30.32
60/40	16.093	10.352	12.747	33.71
50/50	38.665	12.169	12.897	38.52

optical sensor or bandpass filter for the wavelength range of 270–350 nm in the UV–vis region. Figure 12 shows the dependence of the optical band gap energy on the PVDF content in the blend. It is clear that the optical band gap energy increased with increasing PVDF content. The values of the optical band gap energy for blend films of different compositions are listed in Table III. The existence and variation of the optical band gap energy may be explained if we invoke the occurrence of local crosslinking within the amorphous phase of PMMA and PVDF.

Mechanical properties

The mechanical properties may be considered to be the most important of all the physical and chemical properties of polymers from an application point of view. There are many structural factors that determine the nature of the mechanical behavior of materials, such as the molecular weight, crosslinking, branching, crystallinity, crystal size and shape, and molecular orientation. The mechanical properties of the blend films were measured by the study of the stress–strain characteristics. The values of the tensile strength and elongation at break (%) for blends of various compositions were measured and are listed in Table IV. The effects of the PVDF content on the mechanical properties of the PMMA/PVDF blend films are summarized in Figures 13 and 14, respectively. Figure 13 shows that the tensile strength increased as the percentage of PVDF in the blend increased. With the incorporation of 50 wt % PVDF into the blend, the tensile strength was highest, and it increased to about 38.665 (MPa). The enhancement of the tensile strength was reasonably attributed to the high resistance exerted by the PVDF together with the effect of the stretching resistance of the oriented backbone bond of the polymer chain. Similarly, Young's modulus of the PMMA/PVDF blend films also increased with an increase in the PVDF content in the blend films, as shown in Figure 13. Figure 14 shows that the elongation (%) increased with the increase in the PVDF content in the blend film. However, the elongation (%) for the pure PVDF film was 7.292, which was less than the elongation (%) of blend films of other compositions. The data presented here strongly suggest that the mechanical properties of PMMA/PVDF blends depend on the phase morphology as well as the composition. The range of properties exhibited by the PMMA/PVDF blend system is similar to the range of properties of typical materials used as matrices of commercially available dental restorative materials.[39]

Impact strength

The impact strength test is an important tool for studying the toughening effect of polymers and plastics. The impact strength values of PMMA, PVDF, and their blends are listed in Table IV. The influence of the PVDF content on the impact strength of the blends is shown in Figure 15. PMMA is a brittle

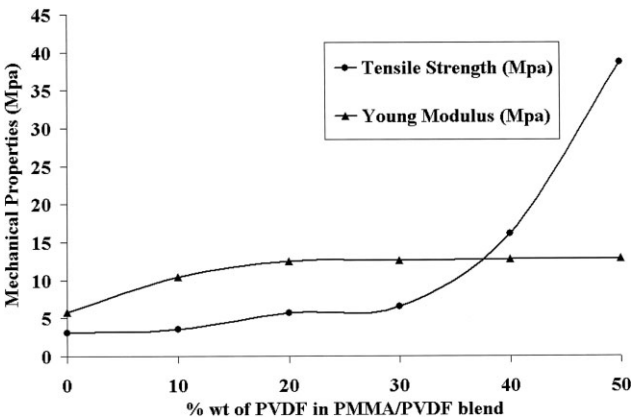

Figure 13 Influence of the PVDF content on the tensile strength and Young's modulus of PMMA/PVDF blend films.

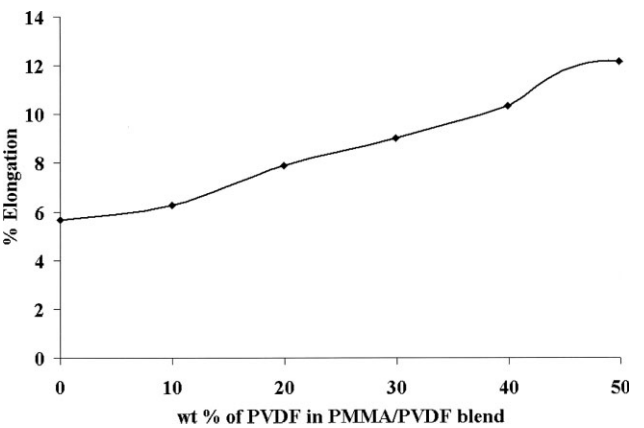

Figure 14 Influence of the PVDF content on the elongation (%) of the PMMA/PVDF blend films.

material and has a notched impact strength of 21.64 J/m. The incorporation of 10–50% PVDF into PMMA enhanced the impact strength of PMMA from 21.64 to 38.52 J/m. The impact strength of the blends was higher than that of pure PMMA. The impact strength increased almost linearly with an increase in the PVDF content. An improvement in the impact strength normally implies a reduction of the stiffness and an increase in the yield strain. A balance between toughness and stiffness is always required for the optimum performance of toughened polymers. It has generally been seen that the optimum dispersion (sufficient compatibility, i.e., neither total miscibility nor complete immiscibility between two components) and adhesion of the rubbery phase with plastics are the basic requirements of impact strength modifications. The chemical nature of the dispersed phase and its compositions decides the dispersibility and adhesion with the continuous phase.[40]

Contact-angle study

The contact angle is an important parameter in surface sciences. It is a regular measure of the surface hydrophobicity that provides information on the hydrophobic or hydrophilic surface at the air–water–solid interface.[41] High contact angles between 70 and 90° indicate strongly hydrophobic surfaces such as those of fluorocarbon polymers, whereas low contact angles (0–30°) indicate highly hydrophilic surfaces such as those of glass and mica.[42] The contact angles against water increased with the PVDF content in the blend films, and this was caused by the hydrophobicity of PVDF due to the CF_2 group of PVDF. The contact angles for blend films of different compositions are listed in Table III. It was believed that the high electronegative properties of the F atom (4.0), the short atom radius (0.135 nm), the shorter C—F bond, and the high bond energy led to the smaller interactions between the molecules of the fluorine-containing polymers. Such properties lead to unique surface properties for fluorine-containing polymers, such as good water and oil repellency, antifouling properties, and good optical properties. Figure 16 shows that the contact angles were larger than 90° when the PVDF content exceeded 30 wt %; this indicated good water repellency. Thus, the contact-angle results indicated that the hydrophobicity against water increased with the PVDF content in the PMMA/PVDF blend films.

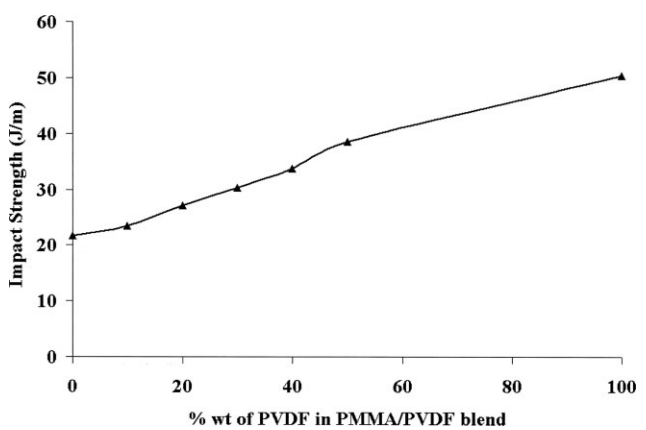

Figure 15 Influence of the PVDF content on the impact strength of the PMMA/PVDF blend films.

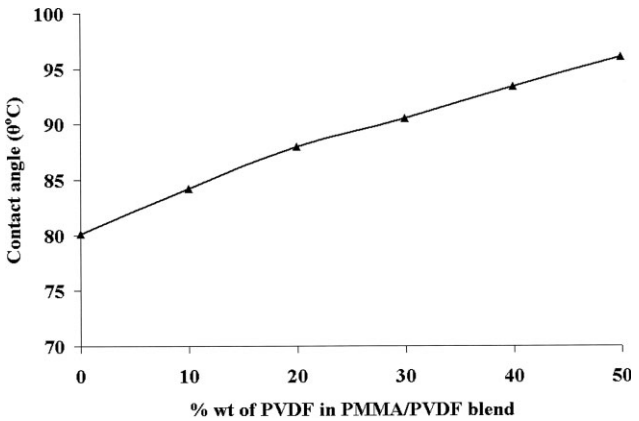

Figure 16 Contact-angle study of the PMMA/PVDF blend films.

CONCLUSIONS

From the FTIR studies, we conclude that the major driving force for the compatibility of these components results from hydrogen bonding involving the carbonyl group of PMMA and the CH_2 groups of PVDF. In light of the DSC and XRD study, we conclude that PMMA/PVDF blends are miscible blends and the two systems are compatible with each other. These results reveal that the crystalline phase of PVDF can be controlled via blending with an amorphous polymer (PMMA) having a specific interaction with PVDF. The tensile strength, elongation (%), and Young's modulus of the blend films increased with an increase in the PVDF content. This shows that PVDF has a strong interaction with PMMA. The enhancement of the mechanical properties was solely due to the reinforcement effect of the dispersed PVDF layers and the intercalated dispersion of PVDF in the PMMA matrix. The impact strength analysis revealed a substantial increase in the impact strength from 21.64 to 38.52 J/m. The change in the UV–vis spectrum was due to complex formation, which could be reflected in the form of a decrease in the optical band gap energy. The contact-angle measurements demonstrated that the hydrophobicity against water increased with the PVDF content in

the blends and that the contact angles against water were larger then 90° when the PVDF content exceeded 30%; this indicated good water repellency. The blends of these two polymers induced disorder of the macromolecules and thus eliminated the high crystallinity of PVDF while maintaining the advantages of the two polymers, such as good water repellency, as shown by the contact-angle study.

The authors express their sincere gratitude to A. K. Kalkar (Department of Physics, University Institute of Chemical Technology, University of Mumbai) for his valuable suggestions and fruitful discussions during this research work. The authors also thank P. K. Das (Indian Rubber Manufacturers' Research Association, Thane, Mumbai, India) for extending the use of the facilities in the laboratory for preparing the blends.

References

1. Poomalai, P.; Ramaraj, B.; Siddaramaiah. J Appl Polym Sci 2007, 106, 684.
2. Ahmed, B.; Habib, I. S. J Appl Polym Sci 2006, 101, 3565.
3. Fang, H.; Mighri, F.; Ajji, A. J Appl Polym Sci 2007, 105, 2955.
4. Brandrup, J.; Immergut, E. H.; Grulke, E. A. Polymer Handbook, 4th ed.; Wiley: New York, 1991; p 49.
5. Brydson, J. A. Plastic Materials, 6th ed.; Butterworth-Heinemann: Oxford, 1995; p 390.
6. Linares, A.; Acosta, J. L. Eur Polym J 1997, 33, 467.
7. Bliznyuk, V. N.; Baig, A.; Singamanemi, S.; Pud, A. A.; Fatyeyeva, K. Y.; Shaporal, G. S. Polymer 2005, 46, 11728.
8. Burke, D. M. J Vinyl Technol 1993, 15, 177.
9. Neuber, R.; Schneider, H. A. Polymer 2001, 42, 8085.
10. Wang, Y.; Kim, D. Electrochim Acta 2007, 52, 3181.
11. Nasef, M. M.; Saidi, H. Mater Chem Phys 2006, 99, 361.
12. Rajendran, S.; Kannan, R.; Mahendran, O. Mater Lett 2001, 49, 172.
13. Gao, Q.; Scheinbeim, J. I. Macromolecules 2000, 33, 7564.
14. Benz, M.; Euler, W. B. J Appl Polym Sci 2003, 89, 1093.
15. Sajkiewicz, P.; Wasiak, A.; Goclowski, Z. Eur Polym J 1999, 35, 423.
16. Gunther, A. M.; Gernot, W.; Reinhold, W. L.; Peter, F. Macromolecules 2005, 38, 6099.
17. Seiler, D. A. In Modern Fluoropolymers, 2nd ed.; Scheirs, J., Ed.; Wiley: Chichester, England, 1998; p 487.
18. Reece, T. J.; Ducharme, S.; Sorokin, A. V.; Poulsen, M. Appl Phys Lett 2003, 82, 142.
19. Coleman, M. M.; Graf, J. F.; Painter, P. C. Specific Interactions and Miscibility of Polymer Blends; Technomic: Lancaster, PA, 1991.
20. Manjunath, B. R.; Venkatraman, A.; Stephan, T. J Appl Polym Sci 1973, 17, 1091.
21. Ramesh, S.; Leen, K. H.; Kumutha, K.; Arof, A. K. Spectrochim Acta A 2007, 66, 1237.
22. Rajendran, S.; Mahendran, O.; Kannan, R. Mater Chem Phys 2002, 74, 52.
23. Ramesh, S.; Lu, S.-C. J Power Source 2008, 185, 1439.
24. Ma, C. C. M.; Chen, C.-H. J Appl Polym Sci 1992, 44, 807.
25. El-Salmawi, K.; Abu Zaid, M. M.; El-Naggar, A. M.; Mamdouh, M. J Appl Polym Sci 1999, 72, 509.
26. Rajendran, S.; Uma, T. Matter Lett 2000, 44, 242.
27. Rajendran, S.; Uma, T. J Power Sources 2000, 88, 282.
28. Brinkhuis, R. H. G.; Schouten, A. J. Macromolecules 1991, 24, 1496.
29. Saikia, D.; Kumar, A. Electrochim Acta 2004, 49, 2581.
30. Rajendran, S.; Mahendran, O.; Mahalingam, T. Eur Polym J 2002, 38, 49.
31. Gregorie, R.; Nociti, N. C. P. S. J Phys D: Appl Phys 1995, 28, 432.
32. Ui, Z.-Y.; Du, C.-H.; Xu, Y.-Y.; Ji, G.-L.; Zhu, B.-K. J Appl Polym Sci 2008, 108, 272.
33. Hideto, M.; Tomofumi, I.; Yoshiro, K. J Appl Polym Sci 2001, 79, 2449.
34. Chunfang, Z.; Baoku, Z.; Genliang, J. J Appl Polym Sci 2006, 99, 2782.
35. Dillon, D. R.; Tenneti, K. K.; Li, C. Y.; Ko, F. K.; Sics, I.; Hsiao, B. S. Polymer 2006, 47, 1678.
36. Buonomenna, M. G.; Macchi, P.; Davoli, M.; Drioli, E. Eur Polym J 2007, 43, 1557.
37. Martin, S.; Stephan, S.; Wehrspohn, B.; Ulrich, G.; Joachim, H. W. Macromolecules 2003, 36, 3646.
38. Enzo, B.; Stefano, C.; Aldo, D. A.; Piergiorgio, V.; Francesco, C.; Mariano, P. Polym Int 1998, 45, 373.
39. Jose, L. G.; Koelling, K. W.; Seghi, R. R. Polymer 1998, 39, 1559.
40. Poomalai, P.; Varghese, T. O.; Siddaramaiah. J Appl Polym Sci 2008, 109, 3511.
41. Tsai, M.-H.; Huang, S.-L.; Chang, P.-H.; Chen, C.-J. J Appl Polym Sci 2007, 106, 4277.
42. Good, R. J. In Contact Angle, Wettability and Adhesion; Mittal, K. L., Ed.; VSP: Utrecht, 1993; p 3.